Seventh International Symposium on Marine Propulsors
smp'22, Wuxi, China, October 2022

Acoustic Emissions and Cavitation Effects on Model Scale Propellers Using a Transition Model*

Jan Geese[1], Julian Kimmerl[1], Marc Nadler[2], Moustafa Abdel-Maksoud[3]

[1]SCHOTTEL GmbH, Dörth, Germany
[2]Faculty of Engineering, Koblenz University of Applied Sciences, Koblenz, Germany
[3]Institute for Fluid Dynamics and Ship Theory, Hamburg University of Technology (TUHH), Hamburg, Germany

ABSTRACT

Transition models are an effective tool for modeling the change of the laminar- and turbulent flow regimes on propeller blades. Thereby, improving the physical accuracy when simulating model scale propellers with a significant fraction of laminar flow. In this study, the influence of the $\gamma - Re_\theta$ transition model, on near-blade cavitation structures and on the underwater-radiated noise is investigated and compared with the frequently used $k - \omega - SST$ turbulence model. For cavitation prediction, the Schnerr-Sauer cavitation model is utilized. The underwater radiated noise is captured by the Ffowcs-Williams-Hawkings acoustic analogy in Kirchhoff formulation. Two propellers in model scale are investigated, the PPTC´11 benchmark propeller VP1304 and the SINTEF P1595 propeller for which experimental acoustic measurements are available. In order to determine a physically feasible transition point, a turbulence intensity parameter study is carried out, based on the critical Reynolds number. Good agreement with the experiments is achieved for both propeller using RANS approaches. Overall, no significant improvements are obtained using the transition model. However, differences are observed in the radiated noise. Thus, indicating that the laminar boundary layer has a noticeable influence on the noise emission.

Keywords

CFD, Transition model, FWH-Method, Cavitation, RANS

1 INTRODUCTION

Underwater radiated noise emissions due to shipping activities are rapidly growing, polluting the marine ecosystem and harming human and animal health and as a secondary effect reducing the comfort of passengers and crew members. One primary source of underwater radiated noise is the propeller. Consequently, there is a growing trend to optimize propellers according to hydroacoustic aspects. Therefore, CFD methods for predicting underwater radiated noise are more and more important. A significant contribution to the noise emission is cavitation in the propeller slipstream, which is triggered by cavities emerging on the propeller blade surface, Therefore the near wall flow regime on propeller blades may significantly affect cavitation behavior and thus noise emission. At model scale, it is often assumed that the flow is fully turbulent and the common RANS turbulence models can be applied, which is not the case in many model test setups, as a significant fraction of flow can still be laminar. Hence, RANS-based transition models are an effective tool for simulating the change of the flow regime on propeller blades from laminar to turbulent flow states. As a result, the physical accuracy is improved in the simulation of propellers in model-scale where Reynolds effects play a role.

Studies conducted from Amadeo et al (2017) show that the $\gamma - Re_\Theta$ transition model is able to improve the computational results compared to the $k - \omega - SST$ turbulence model. In the study conducted by Viitanen et al. (2019) on the influence of the flow transition on the calculated cavitation extent, the results show that the calculated cavitation patterns with and without transition are very similar. However, the influence of the turbulence field quantities on the transition model is not evaluated in the investigation.

In the present study, the influence of the $\gamma - Re_\Theta$ transition model on near-blade flow and cavitation structures and on the underwater radiated noise is evaluated and compared with the frequently used $k - \omega - SST$ turbulence model. For this purpose, two propellers in model scale are investigated. The CFD calculations are validated with open water tests, including cavitation observation and acoustic measurements. In order to localize the physical feasible transition region, a turbulence intensity parameter study is conducted, where the transition region is compared with the critical Reynolds number for lifting surfaces ranging from $0.5 \cdot 10^5$ to $5 \cdot 10^5$ (Sigloch 2017), since the turbulence variables specified, significantly influence the simulation. This approach is akin to the investigation carried out by Baltazar et al (2017), where the laminar regions predicted are compared with paint tests.

2 NUMERICAL METHOD

2.1 Turbulence and Transition Modeling

The turbulence model used in this study is the $k-\omega-SST$ model, which is a modelling approach widely used in solving Reynolds-Averaged-Navier-Stokes (RANS). The $k-\omega-SST$ model is an isotropic turbulence model and follows the Boussinesq hypothesis. In the model, the two variables k and ω are modelled, k is the turbulence kinetic energy and ω is the rate of dissipation of the eddies. The model combines the turbulence models $k-\omega$ and $k-\varepsilon$. While the $k-\omega$ model is used in the inner region of the boundary layer, the $k-\varepsilon$ model is applied in the free shear flow.

Transition is considered by utilizing the correlation based $\gamma-Re_\theta$ transition model. A model in which the $k-\omega-SST$ turbulence model is extended by two additional transport equations, used to determine the laminar-turbulent transition in the boundary layer. The intermittency γ is a quantity for the probability that a certain point is located in the turbulent region of the flow. When γ is unity, the model behaves as the standard $k-\omega-SST$ turbulence model. The momentum thickness Reynolds number Re_θ and turbulence intensity Tu are correlated. The transport equation for the local transition onset momentum thickness Reynolds number $\overline{Re_{\theta t}}$ triggers the intermittency γ.

2.2 Cavitation Modeling

For cavitation modelling, the Schnerr-Sauer cavitation model is utilized. This model is based on a volume of fluid (VOF) method and considered as an Eulerian mixture model (Schnerr & Sauer 2001). Species are viewed as isothermal, immiscible fluids, which share one set of momentum equations. For the cell liquid phase fraction $\alpha = V_l/V_{Cell}$ with the volume of liquid in one cell and the overall cell volume V_{Cell}, one additional transport equation

$$\frac{\partial \alpha}{\partial t} + \nabla \cdot (\alpha \overline{u}) + \nabla \cdot [\overline{u_c}\, \alpha(1-\alpha)] = S_\alpha, \qquad (1)$$

is solved, where $\overline{u_c}$ is the artificial velocity compression term. The model is based on the Rayleight-Plesset equation in order to model cavity bubble growth and collapse. The initial nuclei diameter $d_{nuc} = 1 \cdot 10^{-4}\, m$ and the nuclei concentration $n_0 = 1 \cdot 10^{12}\, m^{-3}$ are user set parameters, which combine stability with a high level of detail (Kimmerl et al 2020).

2.3 Acoustic Evaluation

For acoustic evaluation, the Ffowcs-Williams-Hawkings acoustic analogy in its permeable surface formulation is used, also referred to as Kirchhoff formulation (KFWH) (Francescantonio 1997). Derived from the Navier-Stokes equation it is a sufficient method to calculate noise propagation in an unlimited medium generated for example in turbulent flow fields. In the method, the surface integrals of the pressure perturbations are evaluated on a passive control surface enclosed around the region of interest. In this case, the propeller and the surrounding fluid, since the propeller induced fluid fluctuations in the propeller near field are decisive for radiated noise.

A fast Fourier transformation is performed. To reduce spectral leakage, a Hanning window with the length of the pressure vector is applied. The resulting two-sided spectrum is converted to a single-sided spectrum by multiplying the frequency domain signal with a factor of two. Due to the windowing, the energy content is no longer captured correctly. To compensate this effect, each spectral line of the windowed frequency spectrum is multiplied by a fixed energy correction factor. To obtain a sound pressure level (SPL) in dB, the pressure values p, are related to the reference pressure $p_{ref} = 1 \cdot 10^{-6}\, N/m^2$, for underwater radiated noise. For readability, a moving average filter is applied. If available, the sound pressure in narrowband is compared with experimental measurements in one third octave bands.

3 TEST CASES

Two propellers in model scale, presented in Figure 1, are considered. The first one is the Potsdam propeller test case VP1304 propeller (PPTC), which is designed to achieve stable tip vortex cavitation and exhibit a prominent cavitation behavior overall. The other one is the P1595 propeller, designed by SINTEF Ocean to develop more application oriented tip- and hub-vortex cavitation. For the P1595 experimental cavitation observations, acoustic measurements and open water tests are conducted. The experimentally measured data and the geometry of the P1595 propeller are not publicly available at time of publication, but will be published in the future.

VP1304 P1595

Figure 1: Geometry of studied propellers, pressure side view

For both propellers, the main geometric data is listed in Table 1. The studied operation points, presented in Table 2, are selected on basis of their extensive experimental measurements in combination with a distinct laminar region on the propeller blade, according to the critical Reynolds number, which is a requirement for the investigation of a transition model.

Table 1: Geometric data of investigated propellers

	VP1304	P1595
Diameter	250.00 mm	204.00 mm
Pitch ratio at $0.7R$	1.63	1.19
Chord at $0.7R$	104.17 mm	79.13 mm
Area ratio	0.78	0.63
Skew	18.38 °	42.00 °
Number of blades	5	4

Table 2: Investigated operation points

	P1595	VP1304	
	Case 1	Case 2	Case 3
Advance ratio	0.6	1.019	1.262
Rotational speed $[s^{-1}]$	30.0 s^{-1}	25.0 s^{-1}	15.0 s^{-1}
Reynolds at 0.7R	$1.1 \cdot 10^6$	$1.6 \cdot 10^6$	$1.0 \cdot 10^6$
Cavitation number	1.5	2.0	1.4
K_T (wetted)	0.305	0.387	0.249
$10K_Q$(wetted)	0.536	0.976	0.719
K_T (cavitating)	0.302	0.373	0.206
$10K_Q$(cavitating)	–	0.969	0.631

4 COMPUTATIONAL SETUP

To ensure consistency with the experimental setup, the computational domain for both propellers is modelled as the respective cavitation tunnel and visualized in Figure 2. Local refinements of the tip and hub vortex are not applied. This ensures that the influences of the transition on the acoustics and blade cavitation can be investigated, without taking into account the effects of the vortex induced cavitation in the propeller wake.

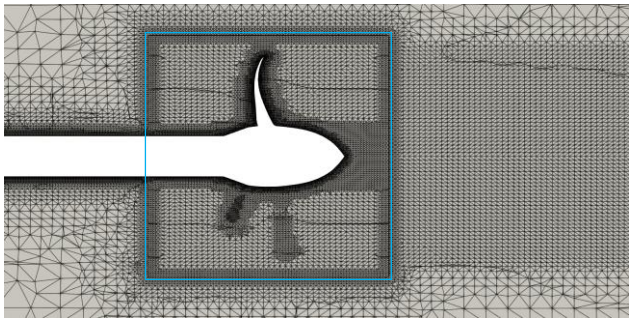

VP1304

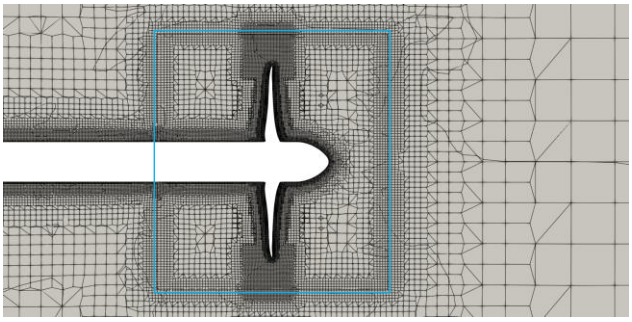

P1595

Figure 2: Domain volume mesh for both propellers, the KFWH control surface is indicated in blue

Since the $\gamma - Re_\Theta$ −transition model is utilized, all grids are modelled with a $y^+ < 1$. Furthermore, it is found that a high amount of prism layers is beneficial for an accurate convergence of global forces (Amadeo et al 2017). Therefore, the amount of prism layers is set to 20. For both propellers, the volume mesh cell count and the number of face cells on one blade are listed in Table 3.

Table 3: Overview of the volume cells and face cells on one blade

	Volume	Blade surface
VP1304	$13.2 \cdot 10^6$	$5.3 \cdot 10^4$
P1595	$11.8 \cdot 10^6$	$1.1 \cdot 10^5$

All calculations are performed transient as full models in order to consider unsteady effects of the flow on the propeller blade. This is necessary for the consideration of cavitation and acoustic aspects in the setups. To account mesh motion, a cyclic AMI boundary condition is applied. Fixed value boundary conditions are set for the inlet velocity and for the turbulence variables. A pressure outlet is utilized, for which the value is set to the corresponding tank pressure taken from the experiment. Except for the transition model, the default values of the turbulence quantities at the inlet are applied $k = 1.5 \cdot 10^{-3}\ m^2/s^2$ and $\omega = 20\ s^{-1}$, since their influence on the $k - \omega - SST$ model is negligible (Baltazar et al 2017).

For all simulations, the OpenFOAM distribution HELYX-Core 3.2.0 is utilized. In order to calculate cavitation with a volume of Fluid (VOF) method, the interPhaseChangeDyMFoam solver is used. For the non-cavitating cases, the cavitation is suppressed by assuming a negative infinite vapour pressure. Thus, no cavitation inception occurs. For cavitating cases, the vapour pressure is raised to the corresponding vapour pressure.

For the measurement of underwater radiated noise from the VP1304 propeller, one near field observer is placed in the domain, with the location at $X = 0.125\,m$, $Y = -0.120\,m$ and $Z = -0.142\,m$. Since no experimental measurements are available, the observer is located close to and outside of the arbitrary mesh interface (AMI).

For the P1595 propeller, acoustic measurements are available. Therefore, one pressure observer is placed at the location of the hydrophone, with the location at $X = 0.035\,m$, $Y = 0.400\,m$ and $Z = 0.128\,m$. The distances for both propellers refer to the simulation origin located at the intersection of the propeller plane and its rotational axis. The right-handed Cartesian coordinate system is defined with the positive X-axis aligned with the propeller rotational axis in flow direction. The gravitational acceleration is applied in negative Z-direction. In order to utilize the KFWH method, it is necessary to span a passive control surface around the acoustic source, from which the surface integrals are evaluated. The control surface is cylindrical and defined at a distance of one millimeter outside from the AMI in the still sufficiently refined mesh, since it is found that this is the only viable location for an accurate evaluation of the acoustic noise. As the dissipation effects are minimized. Due to some limitations in the implementation, it is not possible to position the control surface inside the AMI.

5 TURBULENCE INTENSITY PARAMETER STUDY

The turbulence intensity set at the inlet has a major impact on the transition boundary. Often these quantities are not experimentally measured and therefore an educated guess is necessary. This section summarizes the results of a parameter study, in order to achieve a physically feasible transition point.

Turbulence intensity, implicitly expressed by the turbulent kinetic energy k, can decay substantially from the inlet to the leading edge, depending on the eddy viscosity ratio. The decay is iteratively calculated using the two analytical solutions for (Langtry 2006)

$$\mathrm{k_{inlet}} = \frac{\mathrm{k}}{(1 + \omega_{inlet} \cdot \beta \cdot t)^{-\frac{\beta^*}{\beta}}}, \tag{2}$$

and

$$\omega_{\mathrm{inlet}} = \left(\frac{\rho k_{inlet}}{\mu}\right)\left(\frac{\mu_t}{\mu}\right)^{-1}. \tag{3}$$

Where the constants in the freestream are given by $\beta = 0.09$ and $\beta^* = 0.0828$, which are the default constants from the $k-\omega-SST$ model (Menter 1993). The time scale $t = x/v$, where x is the distance from the inlet to the leading edge and v is the mean convective velocity.

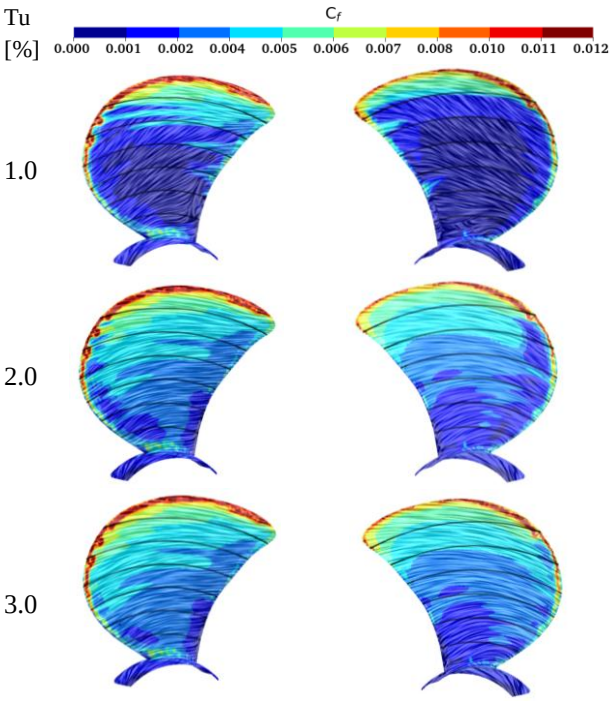

Figure 3: Skin friction coefficient distribution and limiting streamlines over the suction (left) and pressure (right) sides of the VP 1304 propeller at J=1.019 (case 2), calculated by the $\gamma - Re_\theta$-transition model

Based on the results of Baltazar et al. (2017), an eddy viscosity ratio $\mu_t/\mu = 500$ is used in the following investigations. For the VP 1304 propeller, both operation points are simulated using five different turbulence intensities, i.e. $Tu = 0.5\,\%$, $Tu = 1.0\,\%$, $Tu = 1.5\,\%$, $Tu = 2.0\,\%$ and $Tu = 3.0\,\%$, where Tu refers to the target value at the leading edge. It can be clearly recognized that the decay increases with higher turbulence intensities at the inlet. In order to compare the results of the different cases, the skin-friction coefficient distribution and limiting streamlines on the surface of the VP 1304 propeller at *J=1.019* are visualized for the values $Tu = 1.0\,\%$, $Tu = 2.0\,\%$ and $Tu = 3.0\,\%$, see Figure 3. The laminar and turbulent regions can visually be identified. Overall, the laminar region has lower values of friction. Furthermore, at transition, the more radial streamline orientation changes to a more chord wise direction. With increasing turbulence intensity, the turbulent region strongly increases, e.g. at $Tu = 3.0\,\%$ the boundary layer is fully turbulent.

In Figure 4, the physical behavior of the skin friction and the location of the transition point is investigated. The chordwise skin friction coefficient C_f at radius section $r/R = 0.7$ is plotted against the local Reynolds number Re_x. Thus, the transition point, identified by the rapid increase in skin friction, is compared with the critical Reynolds number. Furthermore, the computed C_f values are compared with the Blasius solution for a laminar boundary layer and the Schlichting correlation for a turbulent boundary layer. It is found, that in the present study the turbulence parameters $Tu = 2.0\%$ and

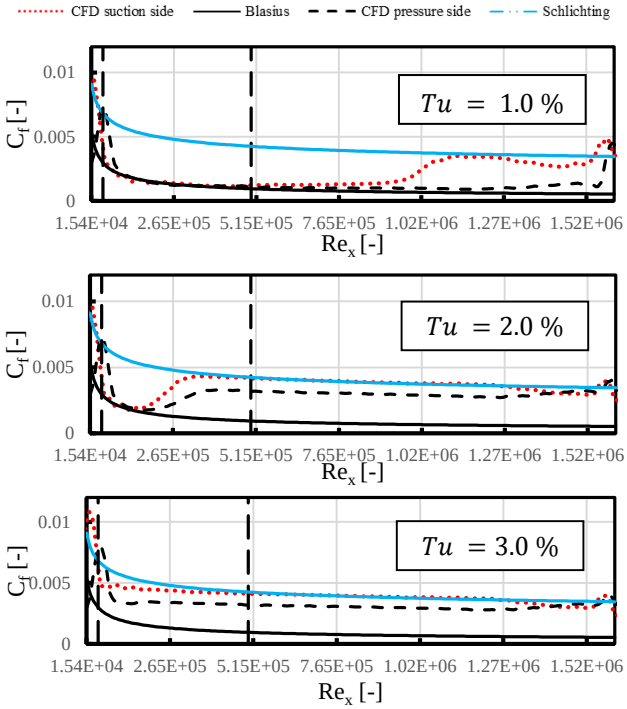

Figure 4: Skin-friction coefficient C_f over Re_x in chordwise direction for $r/R = 0.7$ at J=1.019 (case 2) using the $\gamma - Re_\theta$-transition model. The vertical dashed lines represent the lower and upper range for the critical Reynolds-number.

$\mu_t/\mu = 500$ allow the achieving of simulation results for both operation points of the VP1304 propeller, which are close to the measured data. In general, the skin-friction on the suction side is higher than on the pressure side and matches the results for the Schlichting correlation quite well.

Table 4 includes a comparison between the propeller thrust and torque coefficients with those of the experimental data. The thrust and torque is overestimated in all test cases.

With increasing turbulence intensity, ΔK_T decreases strongly. For the torque coefficient $\Delta 10K_Q$, only slight changes are observed, which does not match the expectation, since the torque should be more affected by the friction distribution. A laminar boundary layer should lead to a more substantial decrease in torque. Overall, the selected inlet turbulence intensity has a significant impact on the prediction accuracy.

Table 4: Difference in K_T and $10K_Q$ compared to the experimental data for different Tu

	Case 2		Case 3	
Tu	ΔK_T	$\Delta 10K_Q$	ΔK_T	$\Delta 10K_Q$
0.5 %	5.68 %	5.72 %	7.90 %	4.77 %
1.0 %	4.84 %	5.38 %	7.86 %	4.85 %
1.5 %	2.94 %	5.24 %	4.72 %	5.04 %
2.0 %	2.56 %	5.18 %	3.47 %	4.93 %
3.0 %	2.27 %	5.18 %	2.20 %	4.83 %

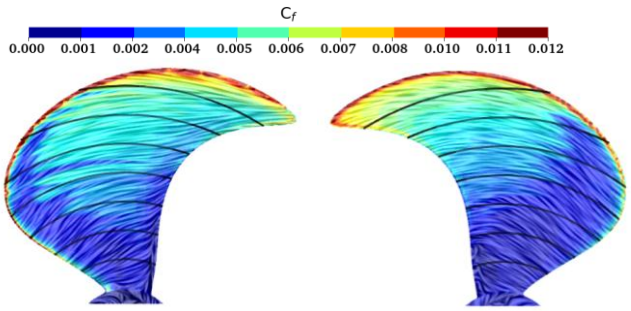

Figure 5: Skin friction coefficient distribution and limiting streamlines representation over the suction (left) and pressure (right) side for the $\gamma - Re_\theta$ -transition model, P1595 propeller (case 1)

The previously determined inlet turbulence variables are applied for the P1595 simulations and presented in Figure 5 and Figure 6. Resulting in a physical feasible transition point.

6 RESULTS

6.1 Global Forces

The following section compares the global forces predicted by the different modelling approaches for each case. For Case 1 and Case 2 cavitating and non-cavitating simulations are conducted. After achieving convergence, the calculated thrust and torque values are averaged over one propeller revolution.

Table 5 includes the differences of the thrust and torque coefficients compared with the measured data. The values are presented for each case and modelling approach. Overall, for the wetted condition, no significant differences in prediction accuracy are evident. Since for the P1595 propeller in cavitating flow condition, no experimental torque measurements are available, the torque is only presented in absolute values and yields a $10K_Q = 0.554$ using the turbulence model without transition. When the transition model is considered, the torque coefficients shows a slight increase ($10K_Q = 0.559$). Furthermore, for case 2 both models show high deviations in the predicted torque coefficients for the cavitating flow condition. Assuming for case 1, that the torque in the experiment changes only slightly when cavitation occurs, then the torque prediction accuracy for the cavitating P1595 is significantly higher when comparing CFD results with the experimental value $10K_Q = 0.536$, for the non-cavitating condition.

Table 5: Comparison between each case and modelling approach, with respect to the experimental data.

	Case 1 (P1595)		Case 2 (VP1304)		Case 3 (VP1304)	
	ΔK_T	$\Delta 10K_Q$	ΔK_T	$\Delta 10K_Q$	ΔK_T	$\Delta 10K_Q$
k-ω SST wetted	0.4%	-1.6%	2.2%	5.0%	2.5%	5.0%
γ-Re$_\theta$ wetted	0.2%	-2.3%	2.6%	5.2%	3.5%	4.9%
k-ω SST cav	-0.3%	–	-0.5%	15.1%	–	–
γ-Re$_\theta$ cav	-2.1%	–	0.9%	15.6%	–	–

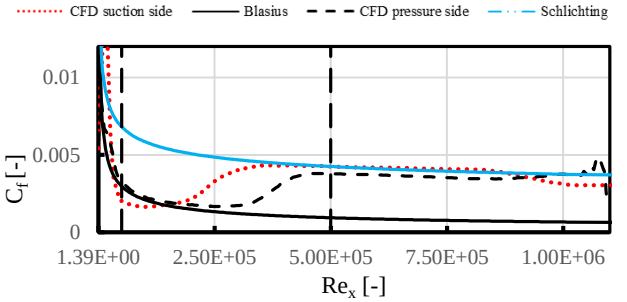

Figure 6: Skin-friction coefficient C_f over Re_x in chordwise direction for $r/R = 0.7$ at using the $\gamma - Re_\theta$ -transition model. The vertical dashed lines represent the lower and upper range for the critical Reynolds-number. P1595 propeller (case1)

6.2 Cavitation Study

In this section, an analysis of the cavitation prediction obtained by the different modelling approaches is given and the results are compared with snapshots taken from the experiments. The cavitation patterns are illustrated as isosurfaces at the interpolated liquid volume phase fraction of $\alpha = 0.5$ and visualized for VP 1304 in Figure 8. The sheet cavitation is overestimated regardless of the simulation model applied. The tip and the root cavitation is captured well by both models, with no significant differences between the modelling approaches. The cavity at the tip slightly extends beyond the tip trailing edge. Due to insufficient mesh refinement in the wake, no tip vortex cavitation develops in the propeller slipstream. The propeller develops a strong hub vortex cavitation, which

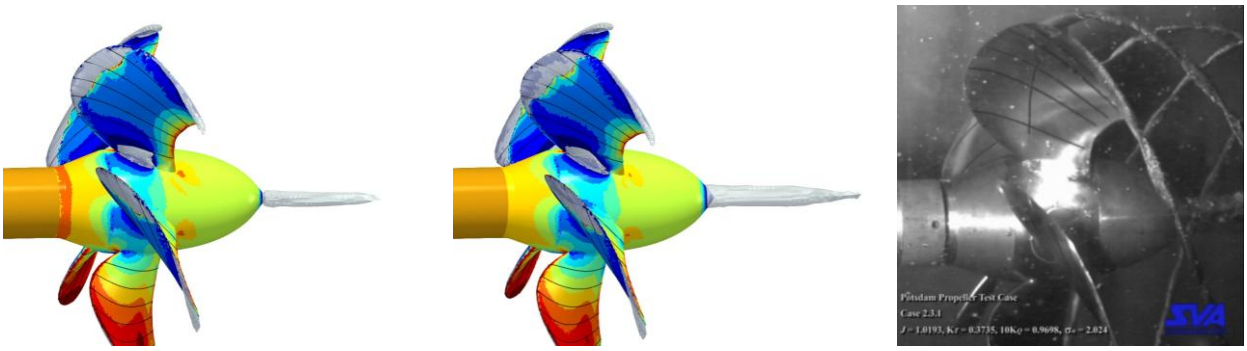

CFD: $\gamma - Re_{\theta}$-transition model CFD: $k - \omega - SST$-turbulence model EFD

Figure 8: Comparison between experimental cavitation observation and liquid volume phase fraction $\alpha = 0.5$ isosurfaces, for the VP 1304 propeller (case 2)

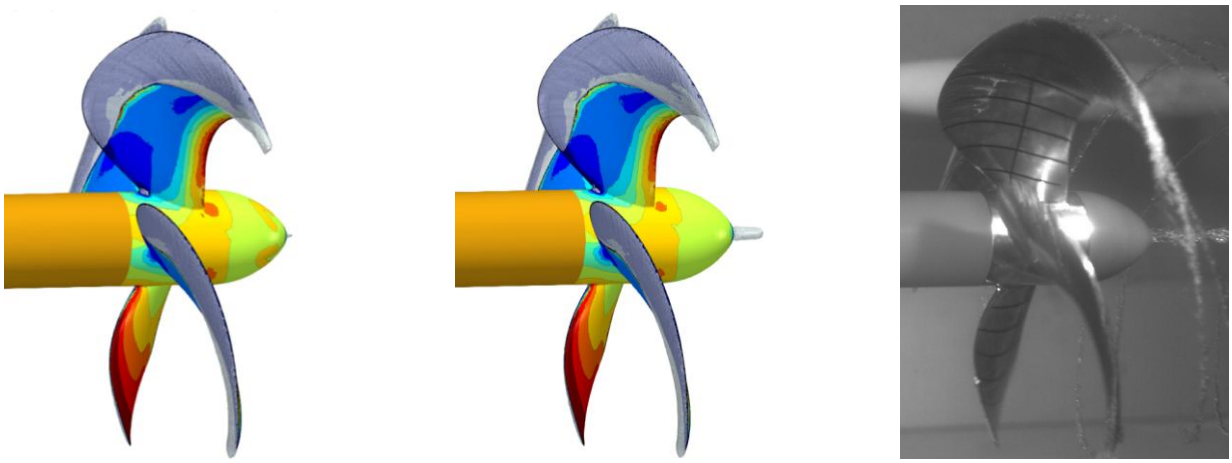

CFD: $\gamma - Re_{\theta}$-transition model CFD: $k - \omega - SST$-turbulence model EFD

Figure 7: Comparison between experimental cavitation observation and liquid volume phase fraction $\alpha = 0.5$ isosurfaces, for the P1595 propeller (case 1)

The $\gamma - Re_{\theta}$ transition model results in a more compact hub vortex cavitation, underpredicting the cavity. This behavior confirms also the results presented in the Viitanen et al (2019) study.

Figure 7 compares the cavitation predicted by the two modelling approaches for the P1595 propeller. The snapshot of the experiment is provided by SINTEF Ocean. Both models overestimate the thin sheet cavitation, occurring in the first quarter of the blade at about a reference radius of $r/R = 0.6$. The cavity at the trailing edge near the tip in the downstream direction is predicted quite well. The $k - \omega - SST$ turbulence model is able to predict the hub vortex cavitation well, contrary to the $\gamma - Re_{\theta}$ -transition model, which follows the trend observed in the VP1304 calculation, where the transition model also captures thinner hub vortex cavitation. Additionally, the transition model shows higher pressure at the hub surface, which can further prevent cavitation inception.

6.3 Acoustic Evaluation

In the following, for the P1595 propeller (case 1), cavitating condition, processed as one-third octave bands. Despite the sound pressure levels (SPL) of the CFD are not

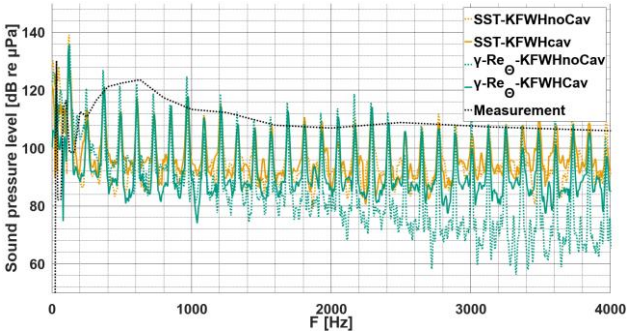

Figure 9: Comparison of sound pressure level obtained from the KFWH method with the experimental data in orange for the $k - \omega - SST$ model, green for the $\gamma - Re_{\theta}$ model. Bold lines for cavitating condition, dotted for wetted condition (case1) P1595 propeller

matching those from the experiment, the trend of the sound pressure is captured quite well by both modelling approaches. Tonal peaks in blade passing frequency are visible. For the $k - \omega - SST$ model no substantial

differences between wetted and cavitating condition are visible. Contrary, the $\gamma - Re_{\Theta}$ model exhibits an increase in SPL for the cavitating condition. which matches the expectation, since cavitation is associated with higher broadband noise emission. The observation for the $k - \omega - SST$ model could be explained by the absence of cavitation excitation as a result of the uniform inflow. Thus, the stable sheet cavitation may be seen as an artificial increase of blade thickness and therefore only affects the blade harmonics. Similar observation for the cavitating tip and hub vortex are documented by Pennings (2016), where oscillation modes of the vortices are not detected in uniform inflow condition and start to appear with a wake grid. .It should be mentioned, that the experimental measurement are in cavitating conditions. Therefore, it is not clear how accurate the models predict the sound pressure in wetted condition. In addition, in this study the cavitating tip vortex is not modelled, which affects the comparability of the results with the experimental data. Overall, the transition model predicts about 5 dB lower sound pressure in cavitating condition, compared to the $k - \omega - SST$ turbulence model.

Figure 10 visualizes the difference between the utilized acoustic analogy and a simple domain pressure probe at observer location for the $k - \omega - SST$ turbulence model. When comparing the cavitating cases, it is evident that the domain pressure probe measures about 5 dB higher sound pressure for many frequencies. Higher and more broadband SPL for frequencies $f < 1000$ Hz are captured by the domain pressure probes in cavitating condition. However, for lower frequencies, the domain pressure probe exhibits no distinct tonal peaks in blade passing frequency.

Figure 11 compares the same for the $\gamma - Re_{\Theta}$ transition model. Similar to the $k - \omega - SST$ turbulence model, the domain pressure probe predicts higher sound pressure in cavitating and wetted condition. Again, the tonal peaks in blade passing frequency are not evident for the domain pressure probe.However, for both methods, the wetted condition predicts less sound pressure in higher frequency ranges, which is expected since cavitation increases the radiated noise.

In general, when comparing the results obtained by the $\gamma - Re_{\Theta}$ transition model with those of $k - \omega - SST$ turbulence model, clear differences can be seen, indicating that the partly laminar region exhibits additional dynamic effects and has a significant impact on noise generation.

The VP1304 propeller is evaluated at $J = 1.019$ (case 2). For this propeller, no experimental measurement are available. Therefore, only the different modelling approaches are compared in Figure 12 utilizing the KFWH method. As for the P1595 propeller, the $k - \omega - SST$ turbulence model predicts higher sound pressure than the $\gamma - Re_{\Theta}$ transition model. Compared to the P1595 calculation, the transition model shows no significant differences between cavitating and wetted condition, maybe due to overall less cavitation present on the propeller blades. For lower frequencies, the $k - \omega - SST$ model predicts higher sound pressure in cavitating condition, which could be a result of the more prominent cavitating hub vortex.

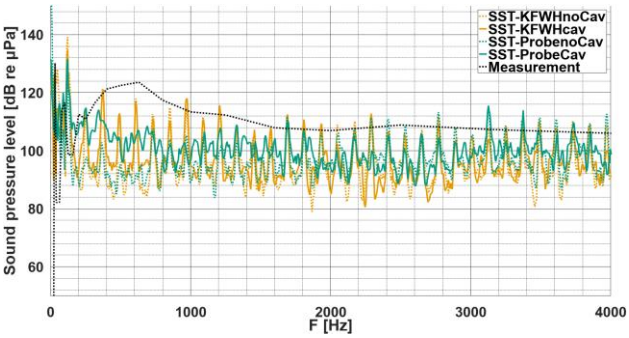

Figure 10: Comparison of sound pressure level obtained from the domain pressure probe (green) and the KFWH method (orange) with the experimental data, bold lines for cavitating condition, dotted for wetted condition, for the $k - \omega - SST$ model, case 1, P1595 propeller

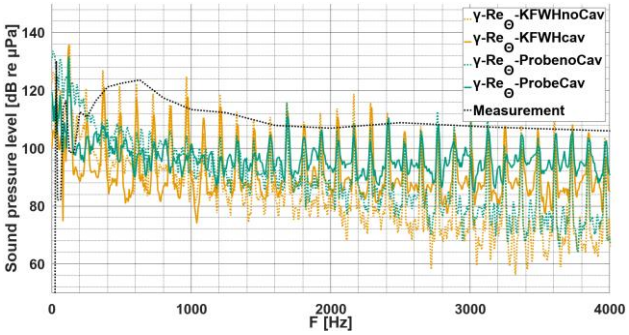

Figure 11: Comparison of sound pressure level obtained from the domain pressure probe (green) and the KFWH method (orange) with the experimental data, bold lines for cavitating condition, dotted for wetted condition, for the $\gamma - Re_{\theta}$ model, case 1 P1595 propeller

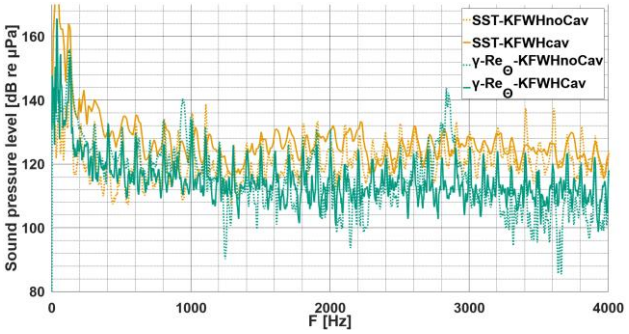

Figure 12: Comparison of sound pressure level obtained from the KFWH method in orange for the $k - \omega - SST$ model, green for the $\gamma - Re_{\theta}$ model. Bold lines for cavitating condition, dotted for wetted condition (case2) VP1304 propeller

7 CONCLUSION

The goal of this work is to investigate the influence of the $\gamma - Re_{\Theta}$ transition model, on the near wall flow field, during model propeller open water tests, including cavitation examination and acoustic evaluation. The results are compared with the $k - \omega - SST$ turbulence model.

Considering the influence of the turbulence inlet quantities on the transition model, the predicted transition point on the propeller blades as well as the predicted loads, depend strongly on the turbulence intensity, defined at the inlet. The turbulent intensity parameter study shows that a turbulence intensity of $Tu = 2.0\%$ at the leading edge in combination with an eddy-viscosity ratio of $\mu_t/\mu = 500$ yields a physically expected location of the transition boundary for all studied operation points. When choosing these turbulence variables, the transition model has no significant impact on the predicted force and thrust. However, a tendency is observed for the transition model to predict less thrust for lower advance ratios compared with $k-\omega-SST$.

Considering the overall propeller cavitation development, the $\gamma - Re_\Theta$ transition model shows no significant improvement and there is no benefit using the transition model when purely optical observations of cavities are required. However, it is observed that the hub vortex cavity is reduced when utilizing the transition model.

In general, the predicted underwater radiated noise using both modelling approaches is fairly in good agreements with the P1595 experimental data, when utilizing the KFWH method and the domain pressure probe. Despite the sound pressure level being different, the trend is captured well.

Furthermore, when utilizing the $\gamma - Re_\Theta$ transition model, significant differences in the radiated noise are observed. Indicating that the laminar boundary layer has a noticeable impact on noise emission. For the P1595 calculation with the $k-\omega-SST$ model, no significant differences between cavitating and wetted conditon are observed, which could be associated with the uniform inflow and indicates that the modelling of the boundary layer transition leads to additional dynamics in the cavitating flow. This suggests the necessity for additional investigation regarding underwater radiated noise with transition models. The influence of the cavitating tip vortex and hub vortex is neglected in this study and it is proposed to consider these cavities in further investigations.

ACKNOWLEDGEMENTS

The authors thank the partners in the ProNoVi project for the support of this work with their contributions to the discussion and the scientific exchange: SINTEF Ocean, CNR-INM, Fr. Lürssen Werft GmbH & Co. KG, Helseth AS. The authors are very grateful for the support and funding by MarTERA, represented by BMWi-project (03SX461C) "ProNoVi" for the German partners.

REFERENCES

Abu-Ghannam, B.J., Shaw, R., (1980). 'Natural Transition of Boundary Layers—The Effects of Turbulence, Pressure Gradient, and Flow History', Journal of Mechanical Engineering Science. 22(5).

Amadeo, M., Juan, G., Mariano, P.; Leo, G. (2017) 'Open Water results comparison for three propellers with transition model, applying crossflow effect, and its comparison with experimental results'. Fifth International Symposium on Marine Propulsors, Espoo, Finland.

Baltazar, J., Rijpkema, D., Falcao de Campos, J. (2017) 'On the Use of the Transition Model for the Prediction of the Propeller Performance at Model-Scale'. Fifth International Symposium on Marine Propulsors, Espoo, Finland.

Barkmann, U. H. (2011). 'Potsdam Propeller Test Case (PPTC) Open Water Tests with the Model Propeller VP1304 Report 3752', Schiffsbau-Versuchsanstalt Potsdam GmbH.

Francescantonio, P. (1997). 'A new boundary integral formulation for the prediciton of sound radiation', Journal of Sound and Vibration. 202(4).

Heinke, H. (2011). 'Cavitation Tests with the Model Propeller VP1304, Report 3753', Schiffsbau-Versuchsanstalt Potsdam GmbH.

Kimmerl, J., Mertes, P., Abdel-Maksoud, M. (2020) 'Turbulence Modelling Capabilities of ILES for Propeller Induced URN Prediction'. SNAME Maritime Convention, Virtual.

Kozlowska, A.N. (2020) 'Cavitation Tests with the P1595 propeller – 302004219, SINTEF Ocean Report No. OC2020F-055, July', SINTEF Ocean.

Langtry, R. B. (2006). 'A correlation-based transition using local variables for unstructured parallelized CFD codes'. [Doctoral dissertation, University of Stuttgart]. Publication Server of the University of Stuttgart, http://dx.doi.org/10.18419/opus-1705.

Menter, F. R., (1993). 'Zonal Two Equation $k-\omega$ Turbulence Models for Aerodynamic Flows', 24th fluid dynamics conference, Orlando, 1993.

Pennings, P. C. (2016). 'Dynamics of Vortex Cavitation'. [Doctoral dissertation, TU Delft]. TU Delft Library, http://doi.org/10.4233/uuid:80840e36-abea-4682-b774-6e826b7f86e0.

Schnerr, G., Sauer, J., (2001). 'Physical and Numerical Modeling of Unsteady Cavitation Dynamics', 4th International Conference on Multiphase Flow, New Orleans, 2001.

Sigloch, H. (2017). Technische Fluidmechanik. 10th ed. Reutlingen: Springer-vieweg.

Viitanen, T., Siikonen, T., Sanchez-Caja, A., (2019). 'Cavitation on Model- and Full-Scale Marine Propellers: Steady and Transient Viscous Flow Simulations at Different Reynolds Numbers', Sixth International Symposium on Marine Propulsors, Rome, Italy